

# Advanced Glycation End Products and Receptor (RAGE) Promote Wound Healing of Human Corneal Epithelial Cells

Christelle Gross,<sup>1</sup> Corinne Belville,<sup>1</sup> Marilyne Lavergne,<sup>1</sup> H el ena Choltus,<sup>1</sup> Matthieu Jabaudon,<sup>1,2</sup> Raiko Blondonnet,<sup>1,2</sup> Jean-Michel Constantin,<sup>1,2</sup> Fr ed eric Chiambaretta,<sup>1,3</sup> Loic Blanchon,<sup>1</sup> and Vincent Sapin<sup>1,4</sup>

<sup>1</sup>Team "Translational approach to epithelial injury and repair", Universit e Clermont Auvergne, CNRS, Inserm, GREd, Clermont-Ferrand, France

<sup>2</sup>CHU Clermont-Ferrand, Department of Perioperative Medicine, Clermont-Ferrand, France

<sup>3</sup>CHU Clermont-Ferrand, Ophthalmology Department, Clermont-Ferrand, France

<sup>4</sup>CHU Clermont-Ferrand, Biochemistry and Molecular Genetic Department, Clermont-Ferrand, France

Correspondence: Vincent Sapin, Bureau n 336, B atiment CRBC, UFR de M edecine et des Professions Param edicales, 28 place Henri-Dunant, BP38, F-63001 Clermont-Ferrand Cedex, France; [vincent.sapin@uca.fr](mailto:vincent.sapin@uca.fr).

**Received:** August 10, 2019

**Accepted:** December 30, 2019

**Published:** March 16, 2020

Citation: Gross C, Belville C, Lavergne M, et al. Advanced glycation end products and receptor (RAGE) promote wound healing of human corneal epithelial cells. *Invest Ophthalmol Vis Sci.* 2020;61(3):14. <https://doi.org/10.1167/iovs.61.3.14>

**PURPOSE.** We used a human corneal epithelial cell (HCE) line to determine the involvement of the advanced glycation end products (AGEs) / receptor for AGEs (RAGE) couple in corneal epithelium wound healing.

**METHODS.** After wounding, HCE cells were exposed to two major RAGE ligands (HMGB1 and AGEs), and wound healing was evaluated using the in vitro scratch assay. Following wound healing, the HCE cells were used to study the influence of the RAGE ligands on HCE proliferation, invasion, and migration. Activation of the nuclear factor (NF)- $\kappa$ B signaling pathway by the AGEs/RAGE couple was tested using a luciferase reporter assay. Functional transcriptional regulation by this pathway was confirmed by quantification of expression of the connexin 43 target gene. For each experiment, specific RAGE involvement was confirmed by small interfering RNA treatments.

**RESULTS.** AGEs treatment at a dose of 100  $\mu$ g/mL significantly improved the wound healing process in a RAGE-dependent manner by promoting cell migration, whereas HMGB1 had no effect. No significant influence of the AGEs/RAGE couple was observed on cell proliferation and invasion. However, this treatment induced an early activation of the NF- $\kappa$ B pathway and positively regulated the expression of the target gene, connexin 43, at both the mRNA and protein levels.

**CONCLUSIONS.** Our results demonstrate that the RAGE pathway is activated by AGEs treatment and is involved in the promotion of corneal epithelial wound healing. This positive action is observed only during the early stages of wound healing, as illustrated by the quick activation of the NF- $\kappa$ B pathway and induction of connexin 43 expression.

**Keywords:** corneal epithelium, RAGE, AGEs, wound healing

Visual acuity is directly correlated with the eye's structural integrity, especially that of the cornea, which is the outer ocular layer. The human cornea is an avascular tissue composed of three layers (epithelium, stroma, and endothelium) separated by two membranes (Bowman membrane and Descemet layer). The cornea is crucial for light refraction to the retina and accounts for three-quarters of the total eye refractive power. However, its anterior localization in the eye means that it must maintain its transparency. Moreover, its integrity is essential because it also constitutes the first barrier against pathogen infections of the ocular surface.<sup>1-4</sup> However, the anatomical localization of the cornea also exposes it to chemical, thermic, and mechanical injuries leading, in some cases, to anatomical loss of the eye.

Reconstruction of the injured corneal surface, particularly the epithelium, is a multifactorial process regulated by cellular mechanisms involving signaling molecules (alarmins, growth factors, and cytokines) released from the remnant epithelium and stromal cells. Overall, the corneal wound healing machinery involves different dynamic processes, beginning with inflammation (including tissue debridement and dynamic changes in cellular adhesion), followed by reepithelialization (including cellular migration and proliferation), and ending with global tissue remodeling. These cellular and molecular steps require careful regulation, coordination, and control.<sup>5-8</sup> Depending on the gravity of the corneal injury, different clinical strategies are proposed, ranging from drug treatments that control inflammation and enhance

reepithelialization to the use of amniotic patches in more severe cases.<sup>9–14</sup>

A better molecular understanding of the different steps in corneal wound healing is still needed. In this context, the receptor for advanced glycation end products (RAGE), identified in 1992 by Neeper et al., is a target of interest because of its involvement in the control of gene transcription during inflammation and reepithelialization processes.<sup>15,16</sup> One recently published paper demonstrated involvement of the RAGE membrane receptor in corneal injury, as RAGE<sup>-/-</sup> mice showed delayed corneal wound healing.<sup>17</sup> This membrane receptor is a multiligand receptor of the immunoglobulin superfamily, and it binds alarmins. The first types of alarmins is the advanced glycation end products (AGEs) formed by the nonenzymatic reaction of reducing carbohydrates with lysine side chains and N terminal amino groups of macromolecules (amino acids, proteins, phospholipids, and nucleic acids) and called Maillard reaction. Beside AGEs, HMGB1 (high mobility group box 1) or S100 proteins (S100A8, S100A9, S100A12, S100B), for example, are also considered as alarmins and so RAGE ligands.<sup>18–21</sup> Activation of the RAGE, in turn, induces the activation of multiple intracellular signaling pathways (such as MAPK, ERK 1/2, JAK/STAT, JNK, Rho-GTPase, and nuclear factor [NF]- $\kappa$ B), which can modulate inflammatory and reepithelialization processes through several mechanisms, including control of cytokine and chemokine release, cell-cell adhesion, and production of matrix metalloproteases and cytoskeletal proteins.<sup>22,23</sup>

Involvement of the RAGE in wound healing has been best documented by studies on the HMGB1 ligand, which is involved in cellular and tissue processes involving keratinocytes, fibroblasts, alveolar epithelium, and skin through its promotion of cell migration and extracellular matrix dynamics.<sup>24–29</sup> The importance of HMGB1–RAGE binding in healing processes has been confirmed by the use of a blocking antibody, resulting in a loss of the wound healing induced by this ligand.<sup>24,26,29</sup> The involvement of signaling pathways activated by the RAGE has also been confirmed by the use of pharmacological inhibitors.<sup>24–26,29,30</sup> The involvement of the RAGE in wound healing has been demonstrated in numerous tissues; nevertheless, little is known about its activation by different ligands in corneal wound healing. In the present study, we used an in vitro scratch assay model, different chemical forms of HMGB1 (totally oxidized, totally reduced, or a mixture of each), and various AGEs (obtained by the Maillard reaction) to investigate corneal cell wound healing. We demonstrated that HMGB1 (irrespective of chemical form) has no effect, as previously demonstrated for this ligand when used as a mixture of its different forms.<sup>17</sup> By contrast, AGEs had a positive influence on cornea epithelial cell wound healing by promoting cell migration, without affecting cell proliferation or invasion. We also demonstrated activation of the NF- $\kappa$ B pathway and the induction of gene expression of the connexin 43 (Cx43) target gene following AGEs treatment.

## METHODS

### Reagents and Antibodies

Cell culture media, cell transfection opti-MEM (1x) medium, epithelial growth factor (PHG0311), fetal bovine serum (FBS), antibiotics (streptomycin, penicillin, and amphotericin B), and PBS were obtained from Fisher Scientific

(Illkirch, France). Dimethyl sulfoxide (D2650), insulin (I9278), Triton (X100), Tween 20 (P9416), and cholera toxin (C8052) were purchased from Sigma-Aldrich (Saint-Quentin-Fallavier, France). HMGB1 (SRP6265, a mixture of different forms) was obtained from Sigma-Aldrich, HMGB1 in reduced form (HM-131) was obtained from HMGBiotech (Milano, Italia), and AGEs (ab51995, obtained by reaction between BSA and glycolaldehyde) were purchased from Abcam (Paris, France). SuperScript IV First-Strand Synthesis System, *Taq* DNA Polymerase recombinant (10342020), Pierce BCA Protein Assay Kit (23225), Lipofectamine 3000 Transfection Reagent (L3000008), and Lipofectamine RNAiMAX Transfection Reagent (13778150) were purchased from Fisher Scientific. LightCycler 480 SYBR Green I Master (04887352001) was provided by Roche (Meylan, France). Anti-RAGE (ab37647) and anti-Connexin 43 (C6219) rabbit polyclonal primary antibodies for immunofluorescence were obtained from Abcam and Sigma-Aldrich. Donkey anti-rabbit-Alexa488 (A21206) fluorescent-coupled secondary antibody was purchased from Fisher Scientific. Anti-RAGE (sc365154) and anti-connexin 43 (sc271837) mouse monoclonal primary antibodies used for western blotting were purchased from Santa Cruz (Heidelberg, Germany). Horseradish peroxidase-coupled secondary goat-anti-mouse antibody (BI2413C) was provided by Abliance (Compiègne, France) and Hoechst (bisBenzimide H 33258) was obtained from Sigma-Aldrich.

### Cell Culture

Human corneal epithelial cells (HCE) transformed with Ad12-SV40<sup>31</sup> were from ATCC (ref: CRL11135). (HCE) cell line was cultured under standard conditions (5% CO<sub>2</sub>, 95% humidified air, 37°C) in DMEM-F12+GlutaMAX I supplemented with 10% FBS, 5  $\mu$ g/mL insulin, 0.1  $\mu$ g/mL cholera toxin, 10 mg/mL streptomycin, 10,000 U/mL penicillin, 25  $\mu$ g/mL amphotericin B, 10 ng/mL epithelial growth factor, and 0.5% dimethyl sulfoxide.

### In Vitro Model of Corneal Wound Healing (Scratch Assay)

Confluent HCE cells cultivated in four-well plates (Fisher Scientific) were manually scraped with a 200- $\mu$ L pipette tip. After three washes with PBS (1 $\times$ ), wounded cells were either left untreated (control) or treated with RAGE ligands: AGEs (10–200  $\mu$ g/mL), HMGB1 (1–100 ng/mL, mix of different forms), and HMGB1 blocked in reduced form (100 ng/mL). Ligands were added in the medium described previously, without FBS, every 24 hours for 48 hours. Wound images were obtained every 12 hours for 48 hours by light microscopy (Zeiss Axio Observer) using a 5 $\times$  objective, and the wound areas were measured using ImageJ software.<sup>32</sup> This experiment was repeated five times (each condition in duplicate).

### Cell Invasion Assay

Cell invasion was assessed with the CytoSelect 24-well cell migration assay (CBA-101-C; 8  $\mu$ m Fluorometric format; Biolabs, London, UK). At 36 hours after scratch wounding, the HCE cells were suspended in a serum-free medium and placed in the upper chamber containing the same treatment as the scratch assay experiment (100  $\mu$ g/mL AGEs). A 500  $\mu$ L

volume of chemoattractant media containing 10% FBS was then added to the lower chamber. After a 24-hour incubation, cells that had passed through the membrane (8  $\mu\text{m}$  pore size) were then dislodged with a detachment solution. Dislodged cells were stained with CyQuant GR Dye (Fisher Scientific) diluted in lysis buffer and quantified by fluorescence measurement at 480 to 520 nm. This experiment was repeated three times (each condition in triplicate).

### Cell Proliferation Assay

At 36 hours after scratch wounding, cells were stained with 5-Bromo-2'-deoxy-uridine (BrdU) using a BrdU Labeling and Detection Kit II (11299964001; Roche Diagnostics). Briefly, HCE cells were incubated with BrdU (10  $\mu\text{M}$ ) for 45 minutes, washed 3 times with PBS, and then fixed with an ethanol fixative solution (50 mM glycine, pH 2, in 70% ethanol) for 20 minutes at  $-20^{\circ}\text{C}$ . After 3 washes in PBS, cells were incubated with an anti-BrdU antibody (1/25) for 60 minutes at  $37^{\circ}\text{C}$ . Cells were washed 3 times with PBS, followed by incubation with an anti-mouse-Ig-alkaline phosphatase (1/25) for 60 minutes at  $37^{\circ}\text{C}$ . The color substrate solution was added to the cells after three washes in PBS, and the bound anti-BrdU antibody was visualized by light microscopy (Zeiss Axio Observer). Proliferation was expressed as the ratio of BrdU-positive cells to the total number of cells. This experiment was repeated three times (each condition in duplicate).

### Small Interfering RNA Transfection of HCE Cells

For scratch assay experiments, RAGE expression was depleted in HCE cells using small interfering RNA (siRNA). HCE cells at 60% to 80% confluence in 4-well dishes were transfected for 36 hours with 100 nM commercial siRNA against the RAGE (M-003625-02; Dharmacon, Lafayette, LA, USA) or with 100 nM of a nonspecific/scrambled siRNA (siRNA control; D-001206-14; Dharmacon) in 187.5  $\mu\text{L}$  opti-MEM (1 $\times$ ) medium mixed with 11.25  $\mu\text{L}$  Lipofectamine RNAiMAX Reagent in 187.5  $\mu\text{L}$  of opti-MEM (1 $\times$ ). Each condition was analyzed as previously described in the "scratch assay" section. For quantitative RT-quantitative PCR experiments, RAGE expression was depleted in 60% to 80% confluent HCE cells plated in 6-well plates by transient transfection for 36 hours with 100 nM of a commercial siRNA against the RAGE or of a nonspecific siRNA in 125  $\mu\text{L}$  of opti-MEM (1 $\times$ ) medium mixed with 7.5  $\mu\text{L}$  of Lipofectamine RNAiMAX reagent in 125  $\mu\text{L}$  of opti-MEM (1 $\times$ ).

### RAGE Overexpression Transfection

HCE cells seeded in 6-well plates were transiently transfected for 24 hours to overexpress the RAGE. Cells were transfected with 1  $\mu\text{g}$  RAGE expression vector (RG204664; Origene, Herford, Germany) in the presence of 125  $\mu\text{L}$  opti-MEM 1 $\times$  and 5  $\mu\text{L}$  p3000 reagent, mixed with 3.75  $\mu\text{L}$  Lipofectamine 3000 reagent in 125  $\mu\text{L}$  of opti-MEM (1 $\times$ ).

### NF- $\kappa\text{B}$ Luciferase Assay

HCE cells at 60% to 80% confluence were seeded in 6-well plates and tested for NF- $\kappa\text{B}$  transcriptional activity with a luciferase assay. Cells overexpressing RAGE (as previously described) were transiently transfected with 50 ng pRL-TK-Luciferase *Renilla* vector (Promega, Charbonnières-les-

Bains, France), 0.5  $\mu\text{g}$  human pGL4-Luciferase Firefly vector containing NF- $\kappa\text{B}$  response element (219077; Agilent, Les Ulis, France), and 200 ng pMEKK (Agilent) in the positive control condition, as already described. After 6 hours of incubation, the medium was changed to complete DMEM/F12, and the cells were either left in medium (untreated) or treated for 45 minutes with AGEs (100  $\mu\text{g}/\text{mL}$ ). Untreated cells served as control. The cells were lysed in lysis buffer for 15 minutes before the Dual-Luciferase reporter assay (E1910, Promega) was performed, according to the manufacturer's instructions. Results were presented as the ratio between the luminescence of luciferase Firefly and *Renilla*. Experiments were repeated four times for positive controls and five times for AGEs treatments (each experiment in duplicate).

### Quantitative RT-PCR and PCR Experiments

Total RNA was extracted from cell cultures using the RNeasyMini Kit (QIAGEN, Courtaboeuf, France), and cDNA was synthesized by reverse transcription from 1  $\mu\text{g}$  of RNA using a SuperScript IV First-Strand Synthesis System for RT-PCR, according to the manufacturer's protocol. PCR reactions were assessed using Taq DNA polymerase, and quantitative RT-PCR reactions were performed (after scratch assay experiments) using LightCycler 480 SYBR Green I Master mix. Transcripts were quantified independently two times for five experiments of AGEs treatment and for six independent experiments for specific silencing of the RAGE; results were normalized using the geometric means of two housekeeping genes (acidic ribosomal phosphoprotein P0 [RPLP0] and ribosomal protein 17 [RPS17]). Primers used for PCR and qPCR are detailed in the Table. All steps were followed in accordance with the MIQE guidelines.<sup>33</sup> Results are expressed as the ratio between AGEs treatment conditions and the untreated group.

### Immunofluorescence Experiments

Immunofluorescence experiments were performed on cryosections (8  $\mu\text{m}$ ) of human corneas and on HCE cells. Cells were fixed with paraformaldehyde (4% in PBS) and then washed with PBS 1x. Corneal tissue was rehydrated in PBS 1x for 10 minutes. Saturation and permeabilization were performed for 2 hours in PBS containing 10% FBS and 0.1% Triton for HCE cells and PBS containing 4% BSA and 0.2% Triton X-100 for tissues, followed by incubation at  $4^{\circ}\text{C}$  overnight with a rabbit polyclonal anti-RAGE antibody (1/100 for cells and 1/40 for tissues) or rabbit polyclonal anti-Connexin 43 antibody (1/100) diluted in the previously mentioned buffer. For experiments of Cx43 labelling during scratch assay, the incubation of the primary antibody was done 12 hours after the scratch realization. Negative control samples were prepared without primary antibody incubation. After 3 washes in PBS, the cells/tissues were incubated with a goat anti-rabbit antibody conjugated to Alexa488 (1/500) diluted in saturation/permeabilization buffer for 2 hours. Nuclear DNA was detected by incubating the cells/tissue with Hoechst (1/10,000) for 10 minutes at room temperature. The slides were washed three times and examined with a fluorescence microscope (Zeiss-LSM800).

### Protein Extraction and Western Blotting

After scraping and centrifugation at 3,000 rpm, HCE cell pellets were washed in PBS. For RAGE western

TABLE. Sequences of Oligonucleotides Used for RT-PCR and RT-quantitative PCR

Genes	Sequence (5'-3')		Product Size (bp)	Accession No.
	Forward	Reverse		
Human Cx43	AGACAGGCTCTGAGTGCCTGAAC	TCCAGCAGTTGAGTAGGCTTG	175	NM_000165.4
Human RAGE	TGTGCTGATCCTCCCTGAGA	TGCAGTTGGCCCTCCTCG	139	NM_001136.4
Human RPLP0	AGGCTTTAGGTATCACCACCT	GCAGAGTTTCCTCTGTGATA	219	NM_001002.3
Human RPS17	TGCGAGGAGATCGCCATTATC	AAGGCTGAGACCTCAGGAAC	169	NM_001021

blots, proteins were extracted using RIPA extraction buffer containing a mixture of protease inhibitors (04693159001; Roche). For Cx43 western blots, protein was extracted using the Plasma Membrane Protein Extraction Kit (Biovision, Clinisciences, Nanterre, France) containing the same mixture of protease inhibitors. A 150- $\mu$ L volume of the kit buffer was added to the pellet, and the mixture was then vortex mixed and placed on ice for 30 minutes. Samples were centrifuged for 10 minutes at 2,600 rpm and 4°C to eliminate cells debris, followed by a second 30-minute centrifugation of the supernatant at 9,700 rpm and 4°C to separate the membranous and cytosolic fractions. Pellets were resuspended in 20  $\mu$ L of the kit buffer, and both fractions were frozen at -20°C. The protein concentration was determined using a BCA protein assay kit. Samples were denatured in a loading buffer containing 3%  $\beta$ -mercaptoethanol at 100 °C for 5 minutes and separated (40  $\mu$ g of total protein per well) on 4% to 15% Mini-PROTEAN TGX Stain Free Gels (BIO-RAD, Marnes-la-Coquette, France). After electrophoresis, proteins were transferred onto nitrocellulose membranes using a semi-dry transfer cell (TransBlot Turbo Transfer System, 1704150; Trans Blot Turbo RTA Midi Transfer Kit Nitrocellulose, BIO-RAD). Nonspecific sites were blocked for 1.5 hours with Tris-buffered saline (TBS) containing 5% nonfat dry milk (blocking solution), then incubated overnight at 4°C with mouse anti-RAGE (1/600), and mouse anti-connexin 43 (1/200) antibodies in blocking solution containing 0.1% Tween 20 (hybridization solution). The membrane, rinsed 3 times with TBS 0.1% Tween 20, was incubated for 2 hours at room temperature with a horseradish peroxidase anti-mouse conjugated secondary antibody (1/5,000) in hybridization solution. After a wash in TBS-0.1% Tween 20, the membrane peroxidase activity was assayed by enhanced chemiluminescence (Clarity Western ECL Substrate, BIO-RAD). The relative intensities of protein bands were analyzed using Image Lab software (BIO-RAD), and the results were presented as a ratio between the protein of interest and the total protein on the same blot. Results are expressed as the means of five independent experiments.

### Statistics

The data were expressed as means  $\pm$  SEM and were arrived at by calculating the average of duplicates or triplicates of independent experiments. After a first nonparametric ANOVA analysis, and when this one is significant, comparison of means was then performed by a nonparametric test (Mann-Whitney) using GraphPad PRISM software (GraphPad Software Inc.). For all studies, values were considered significantly different at \* $P < 0.05$ , \*\* $P < 0.01$ , \*\*\* $P < 0.001$ .

## RESULTS

### HCE Wound Healing Promoted by the “Coupled Ligand/RAGE Receptor” is Ligand Dependent

We tested the influence of HMGB1 on wound healing in corneal epithelial cells by examining the usual dose response (1 to 100 ng/mL) of different forms of HMGB1. As illustrated in Figure 1A (left and right panels), incubation with 100 ng/mL HMGB1 had no effect on wound healing at any dose tested (1 to 100 ng/mL). As the HMGB1 redox state is known to modulate the protein activity (its reduced form, in particular, showing chemoattractant activity), we tested different HMGB1 forms.<sup>34</sup> No effect was observed with either the reduced or the blocked forms of HMGB1 (data not shown). Conversely, scratch assays conducted with AGEs treatment gave varying results. No effect was obtained with concentrations of 10 or 200  $\mu$ g/mL (Fig. 1B left and right panels), whereas a concentration of 100  $\mu$ g/mL clearly showed a positive effect when compared with the untreated control cells. As shown in Figure 1C (left and right panels), this difference became significant from 12 hours to the end of the scratching test (i.e., 48 hours).

We confirmed that the promotion of HCE wound healing triggered by AGEs ligands was RAGE-specific by transfecting HCE cells with siRNA against the RAGE. We observed a 40% decrease in RAGE expression after 36 hours (Supplementary data S1), which was sufficient to reduce the positive action of AGEs treatment on wound healing (Fig. 1D, left and right panels). This decrease in wound healing became significant by 12 hours, where residual wound areas were 2.32 times smaller than in cells transfected with siRNA against the RAGE (73.6% vs. 31.8% of wound healing). At 24 hours, this value was still 18.3% of the residual wound area for cells transfected with siRNA against the RAGE, whereas the scratch wound had totally closed in cells transfected with scrambled siRNA (Fig. 1D, right panel).

### Characterization of the RAGE Pathway and its Functionality in HCE Cells

We confirmed the expression of RAGE mRNA by PCR in human cornea tissues, corneal epithelial cells, and the HCE cell line (Fig. 2A). Immunohistochemistry conducted to localize the RAGE confirmed expression in the epithelium (principally apical localization), weak expression in the stroma, and expression by the HCE cell model (Fig. 2B, left panel). Western blots of HCE cells confirmed the expected size of the RAGE protein (Fig. 2B, right panel).

Based on previously reported results, the activation of the NF- $\kappa$ B signaling pathway is of primary importance for the cellular action of the RAGE receptor.<sup>22,23,35–37</sup> We used an NF- $\kappa$ B reporter gene assay to confirm the functionality of this system by transfection of a pMEKK positive control,<sup>38</sup>

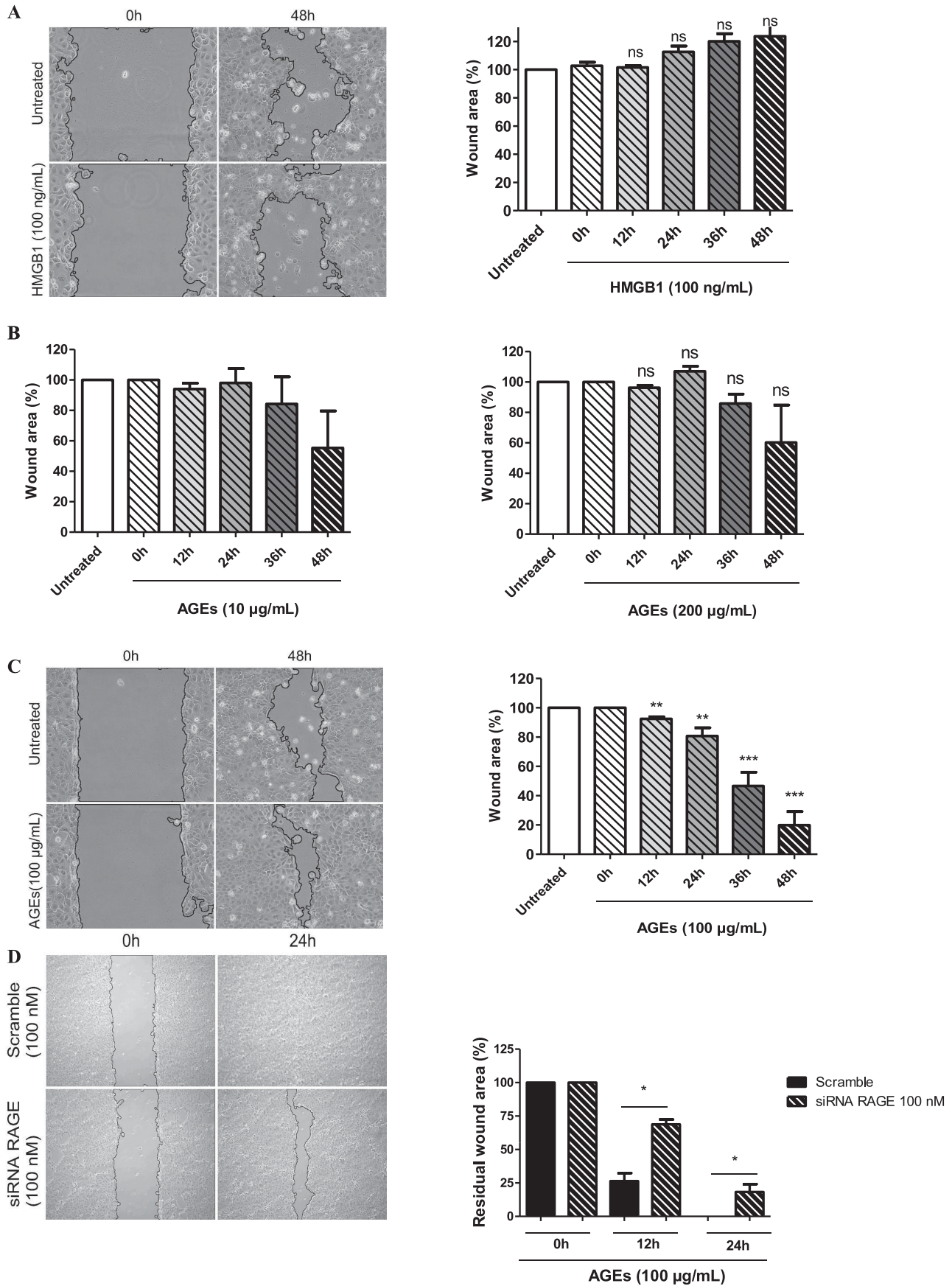


**FIGURE 1.** Involvement of the coupled RAGE ligand/receptor in human corneal epithelial (HCE) cell wound healing. Representative images of scratch assays performed on HCE cells (left panel) treated with HMGB1 (high mobility group box 1, 100 ng/mL) (A) or AGEs (advanced

glycation end products) (10/100/200 µg/mL) (B, C). Percentage of residual wound area (right panel) after treatment with HMGB1 (100 ng/mL) (A) or AGEs (10/100/200 µg/mL) (B, C), compared with 0 hours and standardized to the untreated condition (100%) (n = 5 experiments, each conducted in duplicate). (D) Representative images of scratch assays performed on HCE cells transiently transfected with siRNA against RAGE (siRNA RAGE) or siRNA control (Scramble) (100 nM) for 36 hours and then treated with AGEs (100 µg/mL) (left panel). Percentage of the residual wound area of HCE cells transfected with siRNA against RAGE (100 nM) for 36 hours and then treated with AGEs (100 µg/mL), compared with 0 h (right panel) (n = 5 experiments, each conducted in duplicate). Each bar graph shows mean ± SEM. Mann-Whitney test after a nonparametric ANOVA analysis; \*P < 0.05; \*\*P < 0.01; \*\*\*P < 0.005; ns: not significant.

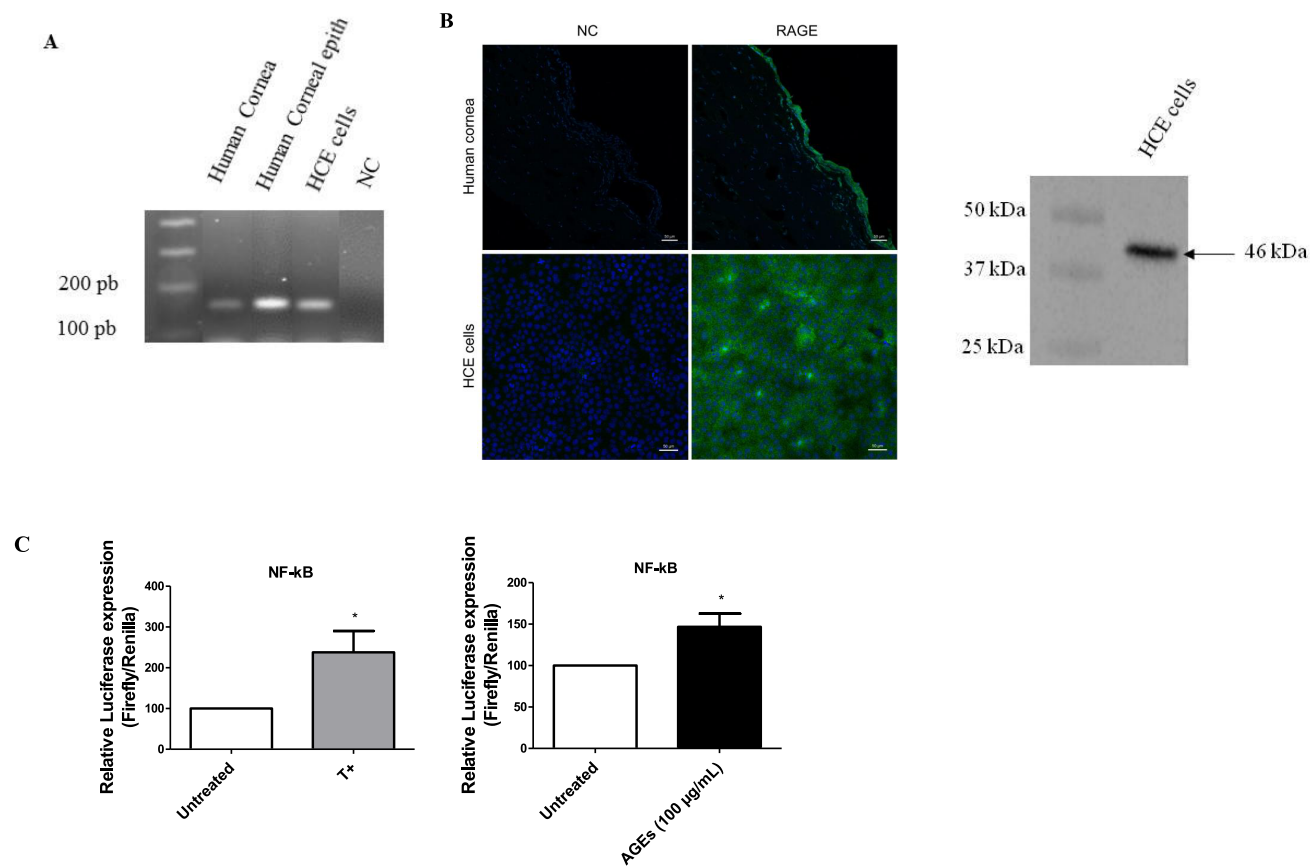


**FIGURE 2.** Functionality of the RAGE pathway. Characterization of the RAGE (A) mRNA and (B) protein expression in human cornea, primary human epithelial cells (mRNA only), and the HCE cell line (mRNA and protein) evaluated by (A) RT-PCR, (B) immunofluorescence, and (B) western blotting. For RT-PCR, negative controls (NC) were performed (A) without cDNA. (B, left panel) Representative images of RAGE expression (green) in human corneas (top panel) and HCE cells (bottom panel). Nuclei were stained with Hoechst (blue); NC (left) were obtained by incubating HCE cells without primary antibody. (B, right panel) Western blot experiments identified the RAGE protein at the described molecular weight (46 kDa). (C) Functionality of the NF-κB pathway (by luciferase reporter gene activity) was measured after treatment of HCE cells with AGEs (100 µg/mL) for 45 minutes (n = 5 experiments, each conducted in duplicate) (right panel). Positive controls (T+) were obtained by co-transfection with pMEKK (n = 5 experiments, each conducted in duplicate) (left panel). Each bar graph shows mean ± SEM. Mann-Whitney; \*P < 0.05.

and we demonstrated an increase in luciferase activity by a factor 2.38 after 45 minutes (Fig. 2C, left panel). A treatment with AGEs, at the same concentration used for the scratch assay (100 µg/mL), resulted in a significant increase in luciferase activity by a factor 1.46 (Fig. 2C, right panel) after 45 minutes.

### AGEs are Involved in Pro-healing Properties in the HCE Cell Line by Promoting Migration Independently of Invasion and Proliferation

Cell invasion, migration, and proliferation are classic events associated with corneal reepithelialization during wound healing. We investigated if AGEs affected one (or several) of

these cellular processes by conducting experiments during scratch assays promoted by AGEs (100 µg/mL). No significant difference was found in cell invasion (Fig. 3A, left panel top and bottom) or cell proliferation (Fig. 3B, right panel top and bottom) until 36 hours, when compared with the untreated condition. Thus, scratch closure is principally from the promotion of cell migration by AGEs treatment, as illustrated previously (Fig. 1C).

### Expression of Cx43, a Target Gene of the RAGE Pathway, is Increased in the Initial Stages of Wound Healing

Cx43 is a well-known target gene of the RAGE pathway, and its expression is described as being modulated during

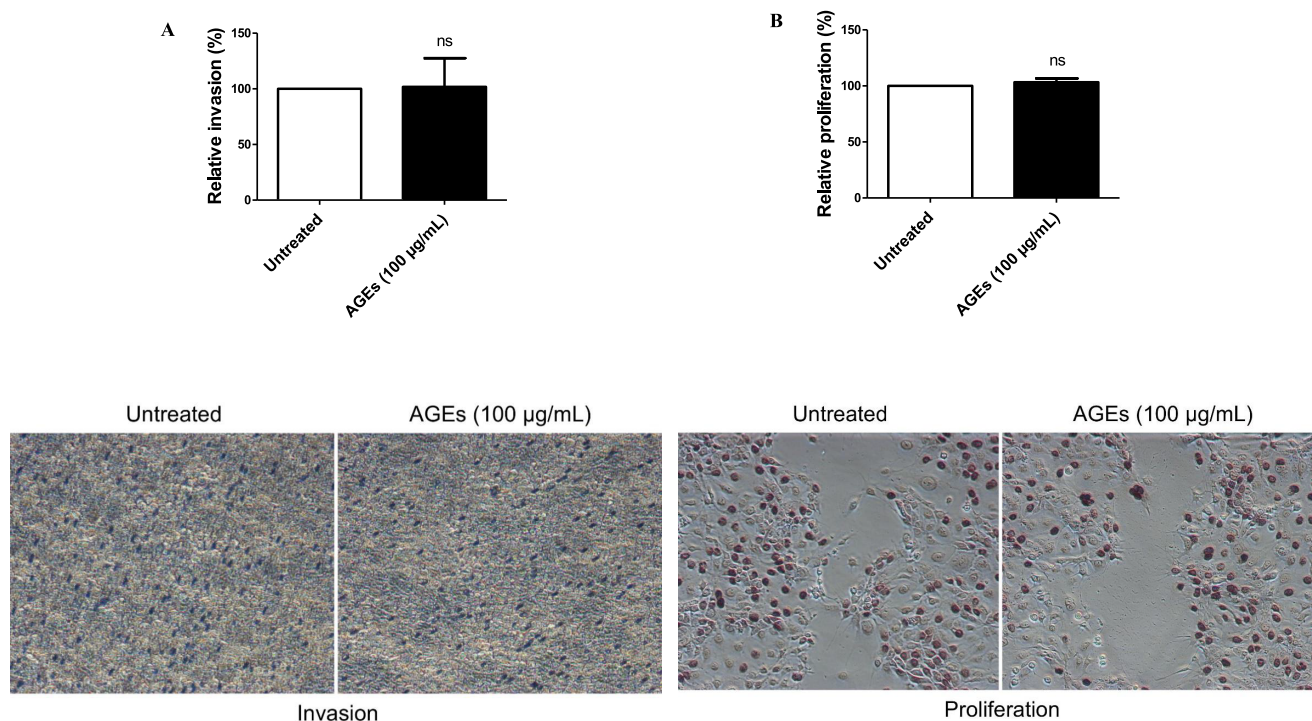


**FIGURE 3.** AGEs treatment positively influenced the pro-healing properties independently of cell invasion and proliferation. Cell invasion and proliferation assays were performed 36 hours after scratch wounding. The percentages of (A) invasion and (B) proliferation were expressed as ratios of cells treated with AGEs (100 µg/mL) to untreated cells (100%) (top panel) ( $n = 5$  experiments, each conducted in triplicate for invasion and duplicate for proliferation). Representative images of noninvasive cells and BrdU labeling proliferative cells are shown in the bottom panel. Each bar graph shows mean  $\pm$  SEM. Mann-Whitney; ns: not significant.

wound healing.<sup>39–51</sup> We first checked and confirmed the basal expression of the Cx43 protein in the human cornea epithelium and in the HCE cell model (Fig. 4A). We then demonstrated that its expression was unchanged by scratch wounding in the absence of a RAGE ligand (Fig. 4B). Treatment with AGEs (100 µg/mL) increased the Cx43 mRNA expression (by 1.5 without scratching and by 3.03 with scratching) at 6 hours, but this increase was partially lost at 24 hours (Fig. 4C, left and right panels). Finally, the direct involvement of the RAGE pathway in Cx43 induction by AGEs (100 µg/mL) was confirmed by transfection with siRNA against RAGE. After 36 hours of RAGE siRNA transfection and 6 hours of AGEs treatment, no induction of Cx43 mRNA expression was observed (Fig. 4C, left panel). Thus, this increase in response to AGEs treatment was confirmed at the protein level by western blot (Cx43 protein levels increased by 2.66 at 12 hours), whereas no induction was noted in the nontreated control condition (in scratch experiments) (Fig. 4D, top and bottom panels). All inductions of protein levels were lost after 24 hours. Results obtained by immunofluorescence demonstrated a time dependent modification of Cx43 protein localization in untreated HCE cells after a wound. Indeed, the initial intracellular staining (t0) with a strong presence in the nucleus became predominant at the cell membrane after 12 hours of culture (t12) (Fig. 4E) (see panel e vs. k). Furthermore, the Cx43 protein distribution was different regarding the distance from the wound (border or internal) (see panel h vs. k). In this case and as expected, the Cx43 protein was less detectable near the wound margins but still present below this frontier (see panel h vs. k). After AGEs treatment (100 µg/mL), Cx43

protein expression near the wound margins seemed to be up-regulated compared with the untreated condition (see panel h vs. n) but followed the same distribution between scratch border and internal cells (see panel n vs. q).

## DISCUSSION

Recovering optimal visual acuity after an injury or trauma (caused, for example, by exposure to harmful chemicals) depends mainly on corneal wound healing. This corneal phenomenon is very complex and involves an intricate dialogue between different cell types (fibroblasts and endothelial and epithelial cells) and many molecular mechanisms.<sup>52</sup> In our present study, we examined classical HCE epithelial cells and used an in vitro scratch wounding assay. We tested the ability of the HCE cells to recover from wounding following activation of the RAGE receptor by two major ligands, called “alarmins”: HMGB1 and AGEs. HMGB1 (a chromatin-associated protein) has recently been demonstrated to undergo relocation to the cytoplasm and is released in stress conditions by corneal epithelial cells. However, the influence of released HMGB1 on human corneal fibroblasts is still unclear, probably due to the lack of TLR2 and TLR4 functional receptors at the plasma membranes of these cells, whereas their expression is evident as mRNA.<sup>53,54</sup> In addition to the TLR2 and TLR4 receptors, the RAGE receptor is also an HMGB1 receptor, and involvement of this ligand in the healing process has been previously described.<sup>24–29</sup> The HMGB1 ligand contains three cysteine residues and can, therefore, exist in different isoforms: fully oxidized, disulfide, and thiol (fully reduced).

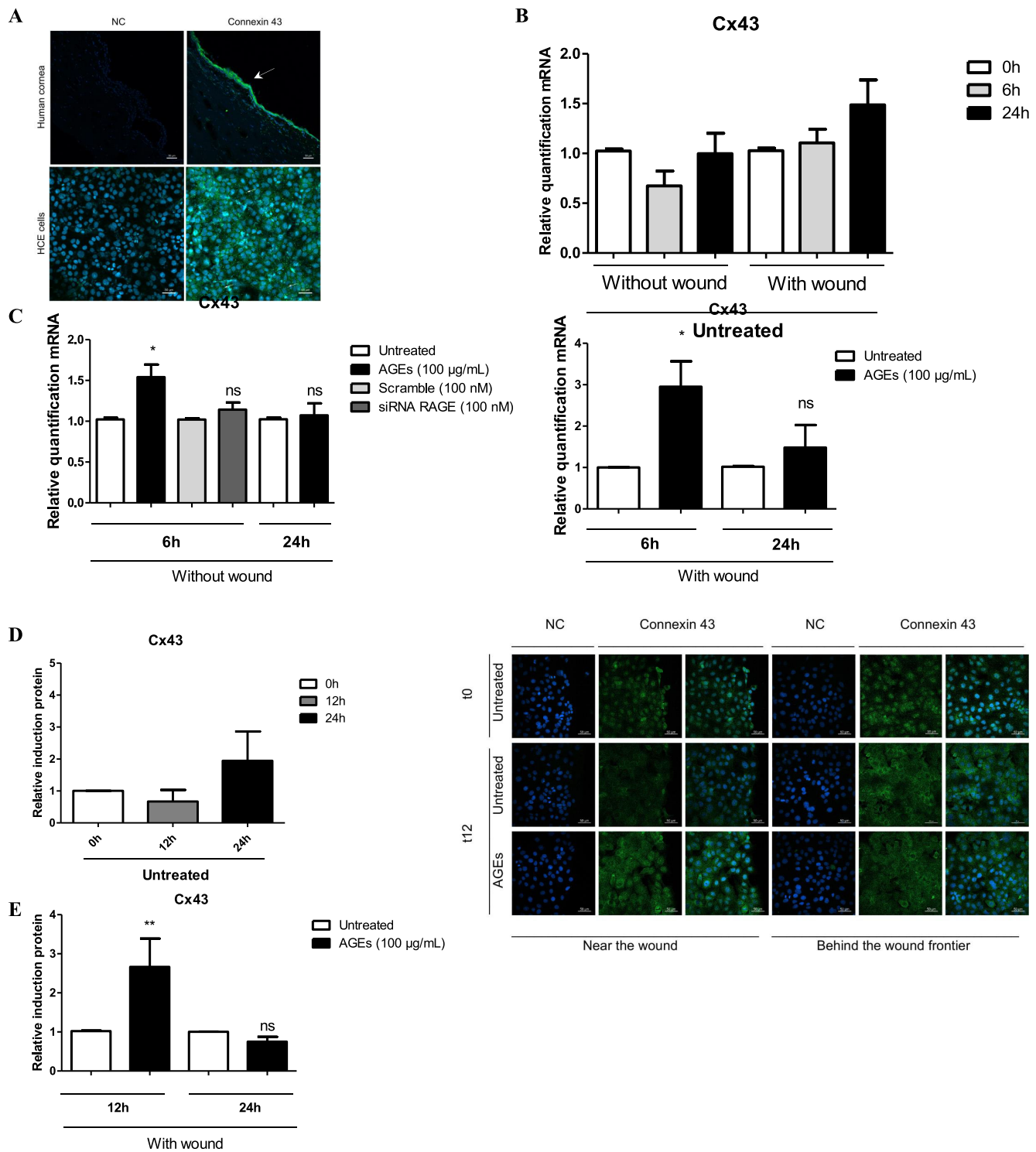


**FIGURE 4.** Cx43 expression is induced by the AGEs/RAGE axis in HCE cells. Characterization of Cx43 protein expression (*arrow*) by immunostaining (bottom panel). Cells incubated without primary antibody served as a negative control (NC). **(B)** Relative quantification of Cx43 mRNA expression in untreated HCE cells 0, 6, and 24 hours after scratch wounding. Results were expressed as a ratio of the 0-hour condition (n = 5 experiments, each conducted in duplicate). **(C)** Quantification of Cx43 mRNA expression in HCE cells treated with AGEs (100 µg/mL) for 6 hours or 24 hours without scratch wounding (left panel) or with scratch wounding (right panel). Cells not treated with AGEs served as a control. Results were expressed as a ratio of the untreated condition at each time point (n = 5 experiments, each conducted in duplicate). (Left panel) Quantification of Cx43 mRNA expression in HCE cells transiently transfected with siRNA against RAGE (siRNA RAGE) (100 nM) for 36 hours and then treated with AGEs (100 µg/mL) for 6 hours. Results were expressed as a ratio of the scrambled siRNA condition (n = 5 experiments, each conducted in duplicate). Each bar graph shows mean ± SEM. Mann-Whitney after a nonparametric ANOVA analysis; \*P < 0.05; ns: not significant. **(D)** Relative quantification of Cx43 protein expression in HCE cells following treatment with AGEs (100 µg/mL) after scratch wounding. Untreated cells served as a control. Results were expressed as a ratio of the 0-hour, unwounded condition (n = 5 experiments) (top panel). Quantification of Cx43 protein expression in HCE cells treated with AGEs (100 µg/mL) for 12 and 24 hours after scratch wounding (bottom panel). Results were expressed as a ratio of the untreated



condition at each time point ( $n = 5$  experiments, each conducted in duplicate) (\*\* $P < 0.01$ ). (E) Characterization by immunostaining of Cx43 protein expression according to the distance from the wound, time, and treatment with AGEs (100  $\mu\text{g}/\text{mL}$ ). Staining of Cx43 protein expression in HCE cells treated near the wound margins (left panel) and behind the wound (right panel). Cells not treated with AGEs (100  $\mu\text{g}/\text{mL}$ ) served as a control. Cells incubated without primary antibody served as a negative control (NC).

These different forms apparently influence its biological activity, as the oxidized form is encountered in noninflammatory states, whereas the thiol HMGB1 isoform is the principal one associated with chronic inflammation.<sup>34</sup> Furthermore, this reduced form has chemoattractant activity, and some studies have confirmed its involvement in wound healing.<sup>27–29</sup> In the present study, we confirmed RAGE expression in the membrane of HCE cells, and then we tested two forms of HMGB1: one composed of the mixture of oxidized, disulfide, and reduced forms classically used in previous published experiments and the other consisting exclusively of a stable and blocked reduced form. Neither form of HMGB1 had any effect on wound healing, in agreement with previous findings by Nass et al., who found no effect of HMGB1 on wound healing in ex vivo mice corneas and who also demonstrated the necessity of the RAGE receptor in the wound healing response.<sup>17</sup> We focused on other RAGE ligands involved in corneal wound healing and conducted similar experiments with AGEs ligands to test their influence on wound healing in our in vitro models. Our AGEs dose-dependency tests confirmed that only a concentration of 100  $\mu\text{g}/\text{mL}$  induced wound healing in HCE cells. This result was somewhat surprising, as most previous publications dealt with diabetes (which is associated with AGEs accumulation and chronic presence), and treatments with “homemade AGEs” typically impaired wound healing.<sup>55–57</sup> Nevertheless, and concomitant with our dose-dependent strategy, we found that a low dose of AGEs (under 100  $\mu\text{g}/\text{mL}$ ) could promote wound healing when used in an acute exposure manner, compared to higher doses, such as 200  $\mu\text{g}/\text{mL}$ , classically used in previous publications. In addition, we also considered that AGEs production was acute during corneal injury (as realized with our model), whereas it would be chronic during diabetes; this difference could potentially modulate the cellular effects of the same regulatory molecule, with potential modifications of RAGE membrane localization or alternative splicing forms expression.

We also showed that the wound repair signaling passed through the RAGE receptor, first by the use of siRNA against the RAGE and second by demonstrating the activation of the NF- $\kappa$ B pathway using a reporter gene approach. However, the influence of the AGEs/RAGE couple on wound healing was not a consequence of changes in cell invasion or proliferation but more of changes in cell migration. To confirm the activation of the RAGE pathways in our model, we focused on an already demonstrated target gene of this pathway, the Cx43 gene.<sup>51</sup> As genes involved in cell–cell junctions, members of the connexin family seem to be good targets for these experiments. Six connexin subunits oligomerize to form a structure called a connexon that is trafficked to and inserted into the plasma membrane.<sup>58</sup> The association of two hemichannels from neighboring cells forms an intercellular gap junction that allows direct intracellular communication through the exchange of small molecules (<1000 Da), including ions, metabolites, and second messengers.<sup>58,59</sup> Gap junctions play important roles in migration, proliferation, differentiation, and inflammation, and connexin family

members are of major importance during wound healing.<sup>60</sup> The expression of the Cx43 protein has been extensively studied with respect to the normal cornea and regarding wound healing.<sup>61–63</sup> In our study, we first confirmed the expression of Cx43 in human cornea (principally in the epithelium) and in HCE cells. We then showed that in the absence of the RAGE ligand, Cx43 expression is still stable 6 hours after scratch wounding, but it is present at a lower level in the scratch wounded condition than in the control unwounded condition. As expected, a 6-hour treatment with AGEs led to an increase in Cx43 expression in our HCE cell scratch wounding model, but this increase did not occur in the presence of siRNA directed against the RAGE. This induction is also present without scratch wounding but to a lesser extent. This molecular induction level reverts to the nontreated level after 24 hours to permit the subsequent steps of wound healing, including cell migration, invasion, and proliferation. Similar results were obtained at the protein level in the scratch wounded condition, with or without AGEs treatment (after 12 hours) and over time (i.e., the response decreased at 24 hours). Taken together, our data for Cx43 expression indicated that the RAGE pathway is activated by AGEs and that the geographical localization of this protein during the scratch must be considered as potentially important to stabilize the cells situated behind the wound. Nevertheless, and specifically concerning the action of Cx43 in wound healing, it could remain controversial because previous publications show either a positive or a negative action of intercellular gap junction proteins in the wound healing process (a variation that could also reflect differences in the cell types examined).<sup>39–50,61</sup> Despite all this, our data clearly indicate that the “RAGE-Cx43” couple is alarmin-dependent and associated with a positive action for the initial steps of healing of an acute injury to the corneal epithelium.

### Acknowledgments

The authors thank Scribendi proofreading services, Canada, for English language editing.

Supported by a Laboratoire Théa grant (CG), a UCA Foundation grant (CG), and a CLARA Auvergne region grant (ML).

Disclosure: **C. Gross**, None; **C. Belville**, None; **M. Lavergne**, None; **H. Choltus**, None; **M. Jabaudon**, None; **R. Blondonnet**, None; **J.-M. Constantin**, None; **F. Chiambaretta**, None; **L. Blanchon**, None; **V. Sapin**, None

### References

1. Eghrari AO, Riazuddin SA, Gottsch JD. Overview of the cornea: structure, function, and development. In: *Progress in Molecular Biology and Translational Science*. Vol 134. Elsevier; 2015:7–23. doi:10.1016/bs.pmbts.2015.04.001
2. Hassell JR, Birk DE. The molecular basis of corneal transparency. *Exp Eye Res*. 2010;91:326–335. doi:10.1016/j.exer.2010.06.021

3. Torricelli AAM, Singh V, Santhiago MR, Wilson SE. The corneal epithelial basement membrane: structure, function, and disease. *Invest Ophthalmol Vis Sci.* 2013;54(9):6390–6400. doi:10.1167/iov.13-12547
4. Goldman JN, Benedek GB, Dohlman CH, Kravitt B. Structural alterations affecting transparency in swollen human corneas. *Invest Ophthalmol Vis Sci.* 1968;7(5):501–519.
5. Eming SA, Krieg T, Davidson JM. Inflammation in wound repair: molecular and cellular mechanisms. *J Invest Dermatol.* 2007;127:514–525. doi:10.1038/sj.jid.5700701
6. Maycock NJR, Marshall J. Genomics of corneal wound healing: a review of the literature. *Acta Ophthalmol.* 2014;92:e170–e184. doi:10.1111/aos.12227
7. Lu L, Reinach PS, Kao WW-Y. Corneal epithelial wound healing. *Exp Biol Med (Maywood).* 2001;226:653–664. doi:10.1177/153537020222600711
8. Saika S, Okada Y, Miyamoto T, et al. Role of p38 MAP kinase in regulation of cell migration and proliferation in healing corneal epithelium. *Invest Ophthalmol Vis Sci.* 2004;45(1):100. doi:10.1167/iov.03-0700
9. Wagoner MD. Chemical injuries of the eye: current concepts in pathophysiology and therapy. *Survey Ophthalmol.* 1997;41:275–313. doi:10.1016/S0039-6257(96)00007-0
10. Sorsby A, Symons HM. Amniotic membrane grafts in caustic burns of the eye. *Br J Ophthalmol.* 1946;30:337–345.
11. Choi JA, Jin H-J, Jung S, et al. Effects of amniotic membrane suspension in human corneal wound healing in vitro. *Mol Vis.* 2009;15:2230–2238.
12. Guo Q, Hao J, Yang Q, Guan L, Ouyang S, Wang J. A comparison of the effectiveness between amniotic membrane homogenate and transplanted amniotic membrane in healing corneal damage in a rabbit model. *Acta Ophthalmol.* 2011;89:e315–e319. doi:10.1111/j.1755-3768.2010.02097.x
13. Joubert R, Daniel E, Bonnin N, et al. Retinoic acid engineered amniotic membrane used as graft or homogenate: positive effects on corneal alkali burns. *Invest Ophthalmol Vis Sci.* 2017;58(9):3513–3518. doi:10.1167/iov.17-21810
14. Sharma N, Kaur M, Agarwal T, Sangwan VS, Vajpayee RB. Treatment of acute ocular chemical burns. *Survey Ophthalmol.* 2018;63:214–235. doi:10.1016/j.survophthal.2017.09.005
15. Neeper M, Schmidt AM, Brett J, et al. Cloning and expression of a cell surface receptor for advanced glycosylation end products of proteins. *J Biol Chem.* 1992;267:14998–15004.
16. Brett J, Schmidt AM, Yan SD, et al. Survey of the distribution of a newly characterized receptor for advanced glycation end products in tissues. *Am J Pathol.* 1993;143:1699–1712.
17. Nass N, Trau S, Paulsen F, Kaiser D, Kalinski T, Sel S. The receptor for advanced glycation end products RAGE is involved in corneal healing. *Ann Anat Anatomischer Anzeiger.* 2017;211:13–20. doi:10.1016/j.aanat.2017.01.003
18. Schmidt AM, Stern DM. Receptor for age (rage) is a gene within the major histocompatibility class III region: implications for host response mechanisms in homeostasis and chronic disease. *Front Biosci.* 2001;6:D1151–60. doi:10.2741/schmidt:10.
19. Schmidt AM, Hori O, Cao R, et al. Rage: a novel cellular receptor for advanced glycation end products. *Diabetes.* 1996;45(Supplement\_3):S77–S80. doi:10.2337/diab.45.3.S77
20. Leclerc E, Fritz G, Vetter SW, Heizmann CW. Binding of S100 proteins to RAGE: An update. *Biochim Biophys.* 2009;1793:993–1007. doi:10.1016/j.bbamcr.2008.11.016
21. Hori O, Brett J, Slattery T, et al. The receptor for advanced glycation end products (rage) is a cellular binding site for amphotericin: mediation of neurite outgrowth and co-expression of rage and amphotericin in the developing nervous system. *J Biol Chem.* 1995;270:25752–25761. doi:10.1074/jbc.270.43.25752
22. Sorci G, Riuzzi F, Giambanco I, Donato R. RAGE in tissue homeostasis, repair and regeneration. *Biochim Biophys.* 2013;1833:101–109. doi:10.1016/j.bbamcr.2012.10.021
23. Xie J, Méndez JD, Méndez-Valenzuela V, Aguilar-Hernández MM. Cellular signalling of the receptor for advanced glycation end products (RAGE). *Cell Signal.* 2013;25:2185–2197. doi:10.1016/j.cellsig.2013.06.013
24. Ranzato E, Patrone M, Pedrazzi M, Burlando B. Hmgb1 promotes wound healing of 3T3 mouse fibroblasts via Rage-dependent ERK1/2 activation. *Cell Biochem Biophys.* 2010;57:9–17. doi:10.1007/s12013-010-9077-0
25. Ranzato E, Patrone M, Pedrazzi M, Burlando B. HMGB1 promotes scratch wound closure of HaCaT keratinocytes via ERK1/2 activation. *Mol Cell Biochem.* 2009;332:199–205. doi:10.1007/s11010-009-0192-4
26. Pittet J-F, Koh H, Fang X, et al. HMGB1 accelerates alveolar epithelial repair via an IL-1 $\beta$ - and  $\alpha$ v $\beta$ 6 integrin-dependent activation of TGF- $\beta$ 1. *PLoS One.* 2013;8. doi:10.1371/journal.pone.0063907
27. Sinagra T, Merlo S, Spampinato SF, Pasquale RD, Sortino MA. High mobility group box 1 contributes to wound healing induced by inhibition of dipeptidylpeptidase 4 in cultured keratinocytes. *Front Pharmacol.* 2015;126:1–9. doi:10.3389/fphar.2015.00126
28. Straino S, Di Carlo A, Mangoni A, et al. High-Mobility Group Box 1 protein in human and murine skin: involvement in wound healing. *J Invest Dermatol.* 2008;128:1545–1553. doi:10.1038/sj.jid.5701212
29. Ojo OO, Ryu MH, Jha A, Unruh H, Halayko AJ. High-mobility group box 1 promotes extracellular matrix synthesis and wound repair in human bronchial epithelial cells. *Am J Physiol.* 2015;309:L1354–L1366. doi:10.1152/ajplung.00054.2015
30. Sakaguchi M, Kinoshita R, Putranto EW, et al. Signal diversity of receptor for advanced glycation end products. *Acta Med Okayama.* 2017;71:459–465.
31. Kahn CR, Young E, Lee IH, Rhim JS. Human corneal epithelial primary cultures and cell lines with extended life span: in vitro model for ocular studies. *Invest Ophthalmol Vis Sci.* 1993;34(12):3429–3441.
32. Schindelin J, Arganda-Carreras I, Frise E, et al. Fiji: an open-source platform for biological-image analysis. *Nat Methods.* 2012;9:676–682. doi:10.1038/nmeth.2019
33. Bustin SA, Benes V, Garson JA, et al. The MIQE guidelines: minimum information for publication of quantitative real-time PCR experiments. *Clin Chem.* 2009;55:611–622. doi:10.1373/clinchem.2008.112797
34. Richard SA, Jiang Y, Xiang LH, et al. Post-translational modifications of high mobility group box 1 and cancer. *Am J Transl Res.* 2017;9:5181–5196.
35. Xie Y, Yu N, Chen Y, Zhang K, Ma H-Y, Di Q. HMGB1 regulates P-glycoprotein expression in status epilepticus rat brains via the RAGE/NF- $\kappa$ B signaling pathway. *Mol Med Rep.* 2017;16:1691–1700. doi:10.3892/mmr.2017.6772
36. Lim S, Lee ME, Jeong J, et al. sRAGE attenuates angiotensin II-induced cardiomyocyte hypertrophy by inhibiting RAGE-NF $\kappa$ B-NLRP3 activation. *Inflammation Res.* May 2018;67:691–701. doi:10.1007/s00011-018-1160-9
37. Zhang J, Shao S, Han D, et al. High mobility group box 1 promotes the epithelial-to-mesenchymal transition in prostate cancer PC3 cells via the RAGE/NF- $\kappa$ B signaling pathway. *Int J Oncol.* Aug 2018;53:659–671. doi:10.3892/ijo.2018.4420
38. Schulze-Osthoff K, Ferrari D, Riehemann K, Wesselborg S. Regulation of NF- $\kappa$ B activation by MAP kinase

- cascades. *Immunobiology*. 1997;198:35–49. doi:[10.1016/S0171-2985\(97\)80025-3](https://doi.org/10.1016/S0171-2985(97)80025-3)
39. Li X, Zhou H, Tang W, Guo Q, Zhang Y. Transient down-regulation of microRNA-206 protects alkali burn injury in mouse cornea by regulating connexin 43. *Int J Clin Exp Pathol*. 2015;8:2719–2727.
  40. Elbadawy HM, Mirabelli P, Xeroudaki M, et al. Effect of connexin 43 inhibition by the mimetic peptide Gap27 on corneal wound healing, inflammation and neovascularization: Connexin 43 mimetic peptide Gap27 for corneal wound healing. *Br J Pharmacol*. 2016;173:2880–2893. doi:[10.1111/bph.13568](https://doi.org/10.1111/bph.13568)
  41. Grupcheva CN, Laux WT, Rupenthal ID, McGhee J, McGhee CNJ, Green CR. Improved corneal wound healing through modulation of gap junction communication using connexin43-specific antisense oligodeoxynucleotides. *Invest Ophthalmol Vis Sci*. 2012;53(3):1130–1138. doi:[10.1167/iovs.11-8711](https://doi.org/10.1167/iovs.11-8711)
  42. Moore K, Ghatnekar G, Gourdie RG, Potts JD. Impact of the controlled release of a connexin 43 peptide on corneal wound closure in an STZ model of type 1 diabetes. *PLoS One*. 2014;9. doi:[10.1371/journal.pone.0086570](https://doi.org/10.1371/journal.pone.0086570)
  43. Moore K, Bryant ZJ, Ghatnekar G, Singh UP, Gourdie RG, Potts JD. A synthetic connexin 43 mimetic peptide augments corneal wound healing. *Exp Eye Res*. 2013;115:178–188. doi:[10.1016/j.exer.2013.07.001](https://doi.org/10.1016/j.exer.2013.07.001)
  44. Homkajorn B, Sims NR, Muyderman H. Connexin 43 regulates astrocytic migration and proliferation in response to injury. *Neurosci Lett*. 2010;486:197–201. doi:[10.1016/j.neulet.2010.09.051](https://doi.org/10.1016/j.neulet.2010.09.051)
  45. Marins M, Xavier A, B Viana N, Fortes F, M Fróes M, Menezes J. Gap junctions are involved in cell migration in the early postnatal subventricular zone. *Develop Neurobiol*. 2009;69:715–30. doi:[10.1002/dneu.20737](https://doi.org/10.1002/dneu.20737)
  46. Elias LAB, Wang DD, Kriegstein AR. Gap junction adhesion is necessary for radial migration in the neocortex. *Nature*. 2007;448:901–907. doi:[10.1038/nature06063](https://doi.org/10.1038/nature06063)
  47. Huang GY, Cooper ES, Waldo K, Kirby ML, Gilula NB, Lo CW. Gap junction-mediated cell–cell communication modulates mouse neural crest migration. *J Cell Biol*. 1998;143:1725–1734.
  48. Cina C, Maass K, Theis M, Willecke K, Bechberger JF, Naus CC. Involvement of the cytoplasmic C-terminal domain of connexin43 in neuronal migration. *J Neurosci*. 2009;29:2009–2021. doi:[10.1523/JNEUROSCI.5025-08.2009](https://doi.org/10.1523/JNEUROSCI.5025-08.2009)
  49. Xu X. Connexin 43-mediated modulation of polarized cell movement and the directional migration of cardiac neural crest cells. *Development*. 2006;133:3629–3639. doi:[10.1242/dev.02543](https://doi.org/10.1242/dev.02543)
  50. Bates DC, Sin WC, Aftab Q, Naus CC. Connexin43 enhances glioma invasion by a mechanism involving the carboxy terminus. *Glia*. 2007;55:1554–1564. doi:[10.1002/glia.20569](https://doi.org/10.1002/glia.20569)
  51. Shaikh SB, Uy B, Perera A, Nicholson LFB. AGEs–RAGE mediated up-regulation of connexin43 in activated human microglial CHME-5 cells. *Neurochem Int*. 2012;60:640–651. doi:[10.1016/j.neuint.2012.02.023](https://doi.org/10.1016/j.neuint.2012.02.023)
  52. Qing C. The molecular biology in wound healing & non-healing wound. *Chin J Traumatol*. 2017;20:189–193. doi:[10.1016/j.cjtee.2017.06.001](https://doi.org/10.1016/j.cjtee.2017.06.001)
  53. Iwatake A, Murakami A, Ebihara N. The expression of matrix metalloproteinases and their inhibitors in corneal fibroblasts by alarmins from necrotic corneal epithelial cells. *Jap J Ophthalmol*. 2018;62:92–100. doi:[10.1007/s10384-017-0541-x](https://doi.org/10.1007/s10384-017-0541-x)
  54. Erdinest N, Aviel G, Moallem E, et al. Expression and activation of toll-like receptor 3 and toll-like receptor 4 on human corneal epithelial and conjunctival fibroblasts. *J Inflammation*. 2014;11:3. doi:[10.1186/1476-9255-11-3](https://doi.org/10.1186/1476-9255-11-3)
  55. Shi L, Chen H, Yu X, Wu X. Advanced glycation end products delay corneal epithelial wound healing through reactive oxygen species generation. *Mol Cell Biochem*. 2013;383:253–259. doi:[10.1007/s11010-013-1773-9](https://doi.org/10.1007/s11010-013-1773-9)
  56. Shi L, Yu X, Yang H, Wu X. Advanced glycation end products induce human corneal epithelial cells apoptosis through generation of reactive oxygen species and activation of JNK and p38 MAPK pathways. Langsley G, ed. *PLoS ONE*. 2013;8:e66781. doi:[10.1371/journal.pone.0066781](https://doi.org/10.1371/journal.pone.0066781)
  57. Ljubimov AV. Diabetic complications in the cornea. *Vision Res*. 2017;139:138–152. doi:[10.1016/j.visres.2017.03.002](https://doi.org/10.1016/j.visres.2017.03.002)
  58. Kumar NM, Gilula NB. The gap junction communication channel. *Cell*. 1996;84:381–388. doi:[10.1016/S0092-8674\(00\)81282-9](https://doi.org/10.1016/S0092-8674(00)81282-9)
  59. Loewenstein WR. Junctional intercellular communication: the cell-to-cell membrane channel. *Physiol Rev*. 1981;61:829–913. doi:[10.1152/physrev.1981.61.4.829](https://doi.org/10.1152/physrev.1981.61.4.829)
  60. Willebrords J, Crespo Yanguas S, Maes M, et al. Connexins and their channels in inflammation. *Crit Rev Biochem Mol Biol*. 2016;51:413–439. doi:[10.1080/10409238.2016.1204980](https://doi.org/10.1080/10409238.2016.1204980)
  61. Brandner JM, Houdek P, Hüsing B, Kaiser C, Moll I. Connexins 26, 30, and 43: differences among spontaneous, chronic, and accelerated human wound healing. *J Invest Dermatol*. 2004;122:1310–1320. doi:[10.1111/j.0022-202X.2004.22529.x](https://doi.org/10.1111/j.0022-202X.2004.22529.x)
  62. Matic M, Petrov IN, Rosenfeld T, Wolosin JM. Alterations in connexin expression and cell communication in healing corneal epithelium. *Invest Ophthalmol Vis Sci*. 1997;38(3):600–609.
  63. Ratkay-Traub I, Hopp B, Zs Bor, Dux L, Becker DL, Krenacs T. Regeneration of rabbit cornea following excimer laser photorefractive keratectomy: a study on gap junctions, epithelial junctions and epidermal growth factor receptor expression in correlation with cell proliferation. *Exp Eye Res*. 2001;73:291–302. doi:[10.1006/exer.2001.1040](https://doi.org/10.1006/exer.2001.1040)